Title

Synergistic inactivation of bacteria based on a combination of low frequency, low-intensity ultrasound and a food grade antioxidant

Authors

Huu, Cuong Nguyen

Rai, Rewa

Yang, Xu

et al.

Publication Date

2021-06-01

DOI

10.1016/j.ultsonch.2021.105567

Ultrasonics Sonochemistry 74 (2021) 105567

Contents lists available at ScienceDirect

Ultrasonics Sonochemistry

journal homepage: www.elsevier.com/locate/ultson

Synergistic inactivation of bacteria based on a combination of low frequency, low-intensity ultrasound and a food grade antioxidant

Cuong Nguyen Huu [a], Rewa Rai [a], Xu Yang [a,1], Rohan V. Tikekar [b], Nitin Nitin [a,c,*]

[a] Department of Food Science and Technology, University of California, Davis, CA, USA
[b] Department of Nutrition and Food Science, University of Maryland, College Park, MD, USA
[c] Department of Biological and Agricultural Engineering, University of California, Davis, CA, USA

ARTICLE INFO

Keywords:
Low-frequency
Low-intensity ultrasound
Propyl gallate
Food grade antioxidant
Synergism
Membrane permeability
Food industry

ABSTRACT

This study evaluated a synergistic antimicrobial treatment using a combination of low frequency and a low-intensity ultrasound (LFU) and a food-grade antioxidant, propyl gallate (PG), against a model gram-positive (*Listeria innocua*) and the gram-negative bacteria (*Escherichia coli* O157:H7). Bacterial inactivation kinetic measurements were complemented by characterization of biophysical changes in liposomes, changes in bacterial membrane permeability, morphological changes in bacterial cells, and intracellular oxidative stress upon treatment with PG, LFU, and a combination of PG + LFU. Combination of PG + LFU significantly (>4 log CFU/mL, $P < 0.05$) enhanced the inactivation of both *L. innocua* and *E. coli* O157:H7 compared to PG or LFU treatment. As expected, *L. innocua* had a significantly higher resistance to inactivation compared to *E. coli* using a combination of PG + LFU. Biophysical measurements in liposomes, bacterial permeability measurements, and scanning electron microscope (SEM)-based morphological measurements show rapid interactions of PG with membranes. Upon extended treatment of cells with PG + LFU, a significant increase in membrane damage was observed compared to PG or LFU alone. A lack of change in the intracellular thiol content following the combined treatment and limited effectiveness of exogenously added antioxidants in attenuating the synergistic antimicrobial action demonstrated that oxidative stress was not a leading mechanism responsible for the synergistic inactivation by PG + LFU. Overall, the study illustrates synergistic inactivation of bacteria using a combination of PG + LFU based on enhanced membrane damage and its potential for applications in the food and environmental systems.

1. Introduction

Low-frequency ultrasound is used in the food industry for diverse applications including homogenization, extraction of bioactive compounds from complex food materials, and cleaning of equipment and surfaces [1]. The key advantage of ultrasound processing is its ability to simultaneously creates micro and macroscale mass transport effects [2]. These effects manifest in the form of mechanical impacts including microstreaming, bubble collapse, turbulence, and localized thermal effects. In addition, bubble collapse during ultrasound processing can generate free radicals that may facilitate chemical reactions [3]. Based on these mechanical effects and chemical impacts, the application of ultrasound for inactivation of bacteria in food systems has been evaluated [2,4,5]. The results of these prior studies suggest that even though low-frequency ultrasound may disrupt cell membranes, the overall effectiveness of ultrasound-induced inactivation of bacteria is limited to 1–2 log in model food systems. To address these limitations, ultrasound technology is often combined with other treatments such as thermal or high-pressure processing to improve inactivation of bacteria [6]. Prior studies have shown that simultaneous combination of ultrasound with thermal treatment or high-pressure processing can achieve 4–5 log bacterial inactivation (4–5 log CFU) [6]. Despite this potential, industrial translation of these concepts has been limited due to various factors including the capital cost of combining existing ultrasound technologies with high pressure or thermal processing. In addition, the negative impacts of thermal and high-pressure processing on the overall quality or texture of food products is also a significant limitation. Therefore, there is an unmet need to improve effectiveness of ultrasound processing for

* Corresponding author at: Robert Mondavi Institute South, Room 2221, Hilgard Ln, Davis, CA 95616, USA.
E-mail address: nnitin@ucdavis.edu (N. Nitin).
[1] Present Address: Nutrition and Food Science Department, California State Polytechnic University Pomona, 3801 West Temple Ave, Pomona, CA 91768, USA.

https://doi.org/10.1016/j.ultsonch.2021.105567
Received 10 December 2020; Received in revised form 26 March 2021; Accepted 15 April 2021
Available online 16 April 2021

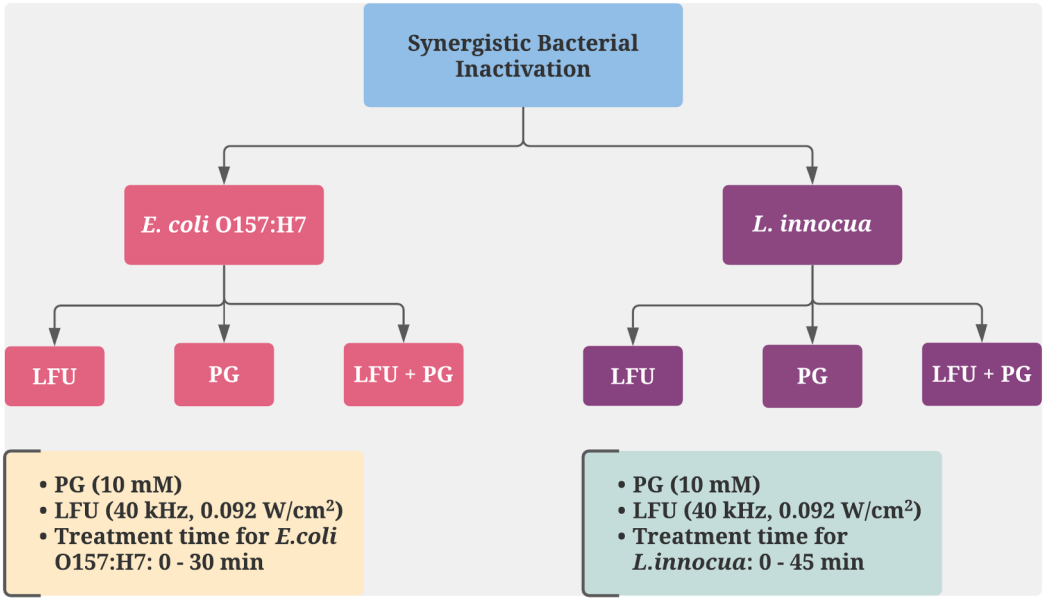

Fig. 1. Experimental design of this current study where LFU – Low-frequency ultrasound treatment, PG – Propyl gallate treatment, LFU + PG – combined Low-frequency ultrasound and PG treatment.

enhancing inactivation of pathogens and spoilage microbes in food systems.

Sonodynamic therapy (SDT) is one of the emerging approaches that is based on a combination of a chemical compound and an ultrasound process to enhance inactivation of diverse types of cells including cancer and bacterial cells [7]. In this concept, a synergistic combination of a chemical compound with the US may result in enhanced chemical and mechanical damage to cells [7–10]. This enhanced cellular damage and inactivation may result due to generation of oxidative stress and membrane damage induced by a combination of US and selected chemical compounds [7,10–13]. Despite these working hypotheses, there are significant gaps in mechanistic understanding of sonodynamic processes that may result in bacterial inactivation. Overall, the sonodynamic inactivation of bacterial cells has a significant potential for the food industry, as the cytotoxic effects of the selected compounds are only limited to ultrasound processing time, unlike other chemical preservatives and additives currently used in the industry. However, most of the currently used compounds for the sonodynamic applications in biomedical systems are not food grade [9]. Thus, the overall goal of this study was to evaluate the synergistic combination of a food-grade compound with a low frequency (40 kHz) and a low power density (0.092 W/mL) ultrasound process to achieve inactivation of bacteria and characterize the role of mechanical damage and oxidative stress for synergistic bacterial inactivation.

In this study, propyl gallate (PG), a derivative of gallic acid (gallate acid propyl ester) was selected as a model food-grade sonosensitizer. Propyl gallate is a well-known antioxidant used in diverse food products, cosmetics, and food packaging materials to prevent rancidity and spoilage. Besides the antioxidant effect, alkyl gallates including PG are reported to have a mild antimicrobial effect against a wide variety of planktonic bacteria, biofilm, and fungi [14–21]. In this study, PG was selected based on its reported membrane activity [22] as well as its ability to generate oxidative stress [17,23] when combined with light irradiation.

In this study, bacterial strains of both the gram-positive (*Listeria innocua*) and the gram-negative bacteria (a non-Shiga toxin-producing *Escherichia coli* O157:H7) representing key foodborne pathogens were selected. Furthermore, the biological changes to cellular membranes and intracellular thiol content were measured in treated bacterial cells to evaluate potential pathways for bacterial inactivation. In summary, this study will illustrate the potential of food-grade compounds with a low frequency and a low-intensity US system (LFU) to achieve synergistic inactivation of target bacteria and characterize the possible mechanisms for this synergistic interaction.

2. Materials and methods

2.1. Reagents

Propyl Gallate (PG), L-α-phosphatidylcholine from egg yolk (egg PC), Reduced L-glutathione (GSH), Sodium Chloride (NaCl), Sodium Dodecyl Sulfate (SDS), Chloroform, Methanol, Ethylenediaminetetraacetic acid (EDTA), and Triton X-100 were all obtained from Sigma-Aldrich (St. Louis, MO, USA). Measure-iT™ Thiol Assay Kit, a thiol-reactive fluorescence probe, was purchased from Molecular Probes (Eugene, OR, USA). 1-hexadecanoyl-2-(1-pyrenedecanoyl)-*sn*-glycero-3-phosphocholine (β-Py-C10-HPC) was purchased from Invitrogen by Thermo Fisher Scientific (Waltham, MA, USA). Zirconia-silica beads (0.1 mm diameter) were acquired from Biospec Products (Bartlesville, OK, USA). Luria-Bertani (LB) broth, Tryptic Soy Broth (TSB), Tryptic Soy Agar (TSA), Phosphate-buffered Saline (PBS), and Tris-hydrochloride (1 M; Tris-HCl) were purchased from Fisher BioReagents (Pittsburgh, PA, USA). Ultrapure water was obtained using a Milli-Q filtration system (EDM Millipore; Billerica, MA, USA).

2.2. Microbial strains, culture methods, and enumeration of bacteria

Escherichia coli O157:H7 (ATCC 700728, Manassas, VA, USA) and *Listeria innocua* (ATCC 33090, Manassas, VA, USA) were provided by Dr. Linda Harris and Dr. Trevor Suslow, respectively, at the University of California, Davis. These strains were selected as models for the gram-negative and gram-positive bacteria respectively. Both bacterial strains have been modified with a rifampicin resistance plasmid, enabling a selective culture of these strains in the rifampicin-containing growth media. Antibacterial experiments were performed against the stationary phase bacteria, at an initial bacterial concentration of 10^6 CFU/mL. Inactivation of bacteria following treatments were assessed based on the standard plate counting method, where treated bacterial samples were serially diluted in a Phosphate-Buffered Saline (PBS) followed by overnight culturing of bacteria on the Rifampicin modified

Tryptic Soy Agar (TSA) plates.

2.3. Study design

To investigate synergistic combination of the combined LFU and PG treatment for inactivation of *E. coli* O157:H7 and *L. innocua*, sample size was determined using a balanced one-way analysis of variance power analysis. For this analysis, the following parameters were selected: number of treatment groups = 4, significance level = 0.05, a power level = 0.8 and f value = 1.2. Based on the power analysis, a sample size of n = 3 for each treatment group was determined.

Briefly, 200 μL of bacterial suspension with a concentration of 1.0×10^7 CFU/mL was added to each well of a round-bottom 12-well plate (Corning, Falcon™, USA) and randomly assigned into four treatment groups.

Group 1. Control without any treatment.

Group 2. PG 10 mM; 200 μL of the bacterial suspension was added to wells containing 2 mL of PG solution at10 mM concentration and then incubated at room temperature for 30 min for *E. coli* O157:H7 and 45 min for *L. innocua* in the dark.

Group 3. LFU; The wells containing bacterial suspension were exposed to ultrasound waves at a frequency of 40 kHz and treatment time ranging from 5 to 30 min for *E. coli*, and from 10 to 45 min for *L. innocua*.

Group 4. LFU + PG; To evaluate the influence of combined treatments based on PG @10 mM and low frequency ultrasound energy. The bacteria suspension was added to the PG solution and immediately exposed to ultrasound.

The detailed experimental design is also illustrated in Fig. 1. The PG concentration was selected based on the solubility limit of the PG in aqueous solution and similar order of magnitude to the allowable limits approved by the FDA for food applications [24].

2.4. Low-frequency and low power density ultrasound treatment (LFU)

A bath sonicator model FB505 (Fisher Scientific, Pittsburgh, PA) was selected as a low-intensity ultrasound process with a frequency of 40 kHz and a power density of (0.092 W/mL) for this study. This system was selected as it can be easily scaled up compared to probe-based US systems. During the process, the temperature of the water was monitored and kept at room temperature by continuously adding cold water. Samples (100 μL) were aseptically collected as a function of treatment time and serial dilutions (1:100 and 1:1000) were prepared using PBS (Fluka Analytical, St. Louis, MO). A volume of 100 μL of each dilution was inoculated onto antibiotic modified TSA plates in triplicates. In order to reduce the detection limit to 1 CFU/mL, the entire volume of the first dilution (1 mL) was also inoculated onto TSA plates (333 μL per plate). TSA plates were incubated at 37 °C for 24 h, and the viable bacterial count was determined.

2.5. Microbial inactivation kinetics

Microbial inactivation kinetics was determined by log-linear regression analysis using GInaFit, an add-in Excel component that was released by Geeraerd et al. [25]. The log-linear equation is a first-order inactivation kinetics that is commonly used to describe inactivation of the bacteria [26].

$$LnN = LnN_0 - kt$$

where N and N_0 are respectively cell count over time and the initial cell count; t is the time (minutes) and k is the inactivation rate constant.

2.6. Membrane damage

2.6.1. Preparation of model lipid membrane with and without pyrene labeled lipid

To understand the influence of PG, LFU, and their combination on bacterial membranes, biophysical changes in liposomes, a model system for the bacterial membrane, were evaluated. These biophysical changes were measured based on changes in the particle size, ξ potential, and lateral membrane mobility in liposomes. Changes in the particle size and ξ potential of liposomes can suggest lysis of the liposomes and the surface interactions of the liposomes with PG and LFU. Lateral mobility measurements can assess changes in the membrane fluidity induced by interactions of PG and LFU with liposomes. Briefly, Egg PC (2.5 mg/ml) with and without 1 mol % of pyrene labeled lipid [1-hexadecanoyl-2-(1-pyrenedecanoyl)-*sn*-glycero-3-phosphocholine (β-Py-C10-HPC)] was dissolved in a mixture of chloroform and methanol (4:1 v/v). The solvent was evaporated under vacuum and dried lipid film was resuspended in an autoclaved water to prepare multilamellar vesicles. Lipid solution underwent extrusion for 15 cycles through 400 nm polycarbonate track-etched membranes to obtain unilamellar vesicles with and without pyrene label.

Size distributions (nm) and ξ potentials (mV) of the liposomal model cell membranes were measured after treatment with PG (10 mM), LFU (30 min), and a combination of PG and LFU using a dynamic light scattering system (Malvern Zetasizer Nano, Westborough, MA). Both treated and untreated samples were diluted 10-fold in 1 × PBS. Polystyrene cuvette with a standard path length of 10 mm and reusable capillary zeta cells was used for size distribution and ξ potential measurements, respectively. Solutions were equilibrated at 25 °C for 2 min before data acquisition. The scattered light was detected at 90° relative to the incident laser (633-nm He-Ne laser) light for 15 to 20 runs of 10 to 20 s each, with a medium viscosity of 0.89 Pa.s and a refractive index of 1.33.

2.6.2. Measurement of lateral mobility using pyrene labeled liposomes

Pyrene labeled probes have been used to measure the lateral mobility of lipid membranes based on the ratio of fluorescence intensity of excimer (470 nm) to monomer (390 nm) peak. Fluorescence emission spectra of liposome model cell membranes labeled with β-Py-C10-HPC (λ_{ex} = 340 nm; λ_{em} = 350 – 600 nm) were acquired using SpectraMax® M5 Multi-Mode Microplate Reader. The instrument was equipped with a Xenon flash lamp (1 J/flash) as an excitation source with two holographic diffraction grating monochromators as wavelength selection devices and a photomultiplier tube as the detector. Emission spectra of β-Py-C10-HPC were acquired using pyrene labeled liposome after treatment with PG (10 mM), ultrasound (30 min), and a combination of both LFU + PG. Treated and untreated control samples were 5-fold diluted with 1 × PBS before fluorescence measurements. Spectral response from appropriate control samples was subtracted before the data analysis. The ratio of the intensity of excimer (470 nm) to monomer (390 nm) peak were calculated to evaluate the change in lateral mobility of liposomal membrane induced by interactions of PG, LFU, and PG + LFU with the membrane.

2.6.3. Propidium iodide dye assay

To measure the magnitude of membrane damage after ultrasound treatment, Propidium Iodide (PI) dye was used for staining the DNA of membrane compromised bacteria as previously described [23]. PI is a red-fluorescent nuclear and chromosome counterstain that can only permeate bacteria with damaged membranes and is frequently used to detect cell membrane damage [27,28]. Test solutions consisting of bacteria (~1×10^9 CFU/mL) suspended in PG solution (10 mM), were treated with ultrasound as described previously. Bacteria in DI water alone in the dark was used as a control. After treatment, samples were washed with DI water and centrifuged for 2 min at 10,000 *g*. Then, a volume of 50 μL of PI was added to each sample to reach a final

concentration of 5 μM, following incubation in the dark at room temperature for 15 min. Subsequently, the incubated samples were washed and suspended in 500 μL 1 × PBS. A volume of 100 μL of this sample was transferred to a 96-well plate, and the fluorescence intensity was measured using a plate reader (Tecan SPECTRAFluor Plus) with an excitation and emission wavelength of 488/520 nm respectively.

2.6.4. Scanning electron microscope (SEM)

Bacterial cells before and after treatment were fixed in 4% glutaraldehyde solution in PBS (pH 7.4) at 4 °C for 2 h and washed twice using Milli-Q water. Ten microliters of samples were then dropped onto aluminum stubs with a carbon conductive adhesive tape, air-dried for 30 min, and sputter-coated with 10 nm of gold. Microscopy was performed on a Philips XL-30 electron microscope with a 10 kV accelerating voltage.

2.7. Oxidative damage

2.7.1. Total intracellular thiol oxidation

Reduction in the intracellular thiol content of *E. coli* O157:H7 *and L. innocua* cells upon individual and combined treatments was evaluated according to the method proposed by Wang et al. [23]. The intracellular thiol-containing compounds were extracted by lysing the bacterial cells through bead beating. First, 1 mL of each sample containing 1×10^9 CFU mL^{-1} of *E. coli* O157:H7 *or L. innocua* were exposed to low-frequency ultrasound treatment, as previously described. Following treatments, the samples were centrifuged (10,000 *g*; 10 min) and the bacterial pellet was resuspended in 500 μL of a sterile lysis buffer (Tris-HCl 50 mM, NaCl 25 mM, EDTA 25 mM, SDS 2%, Triton X-100 1%) and transferred into a sterile 1.5 mL tube containing 400 μL of zirconia-silica beads (0.1 mm). The bacterial suspension was vortexed for 10 min and then centrifuged (16,000 × g; 10 min) before recovering the supernatant. This supernatant was used for the total thiol content measurement. The total thiol content was quantified through fluorescence spectroscopy using the Measure-iT™ Thiol Assay Kit from Molecular Probes (Eugene, OR, USA). The fluorescence intensity was measured using a fluorescence plate reader (Tecan SPECTRAFluor Plus) using an excitation filter of 488 nm and an emission filter of 520 nm. The total thiol content (μM) was determined using a standard curve based on the known concentration levels of reduced glutathione (GSH). The results were expressed in terms of remaining thiol concentration (%) compared to the untreated bacterial sample (Control).

2.7.2. Antioxidant assay

To further confirm the contributions of ROS for the antimicrobial synergistic interaction between PG and ultrasound treatment, two different antioxidants, glutathione and thiourea were exogenously added to the bacterial sample solutions before ultrasound treatment at a concentration of 10 and 100 ppm respectively. These concentration levels were selected based on the previous studies evaluating the role of reactive oxygen species in cell death [28-32]. Both glutathione and thiourea are known scavengers and potent antioxidants. These compounds can prevent damage to important cellular components caused by reactive oxygen species such as free radicals, peroxides, lipid peroxides, and heavy metals by directly scavenging free radicals through the donation of hydrogen atoms mechanism.

2.8. Data analysis

All data were presented as mean ± standard deviation and all experiments were performed in triplicates. Statistical analysis was conducted using a one-way ANOVA and the pairwise differences were evaluated using the Tukey's range test to identify significant differences between each sample group. The difference between the results was considered significant if the P-value was<0.05.

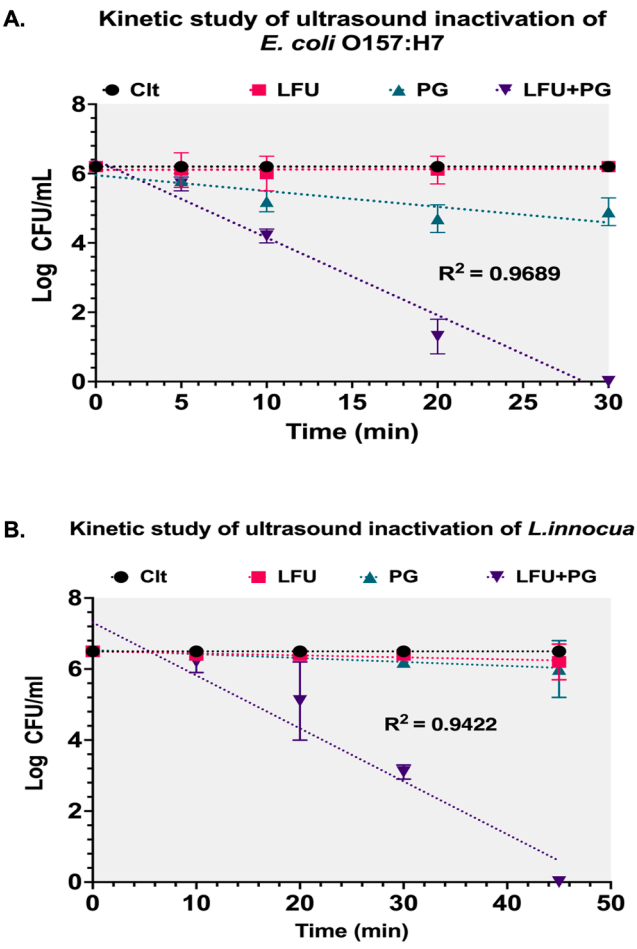

Fig. 2. Inactivation kinetics of *E. coli* O157:H7 *(A) and L. innocua (B)* upon treatment with LFU – Low-frequency ultrasound treatment, PG – Propyl gallate treatment, LFU + PG – combined Low-frequency ultrasound and PG treatment.

3. Results and discussion

3.1. Inactivation kinetics of E. Coli O157:H7 and L. Innocua by low-frequency ultrasound (LFU)

Fig. 2 shows inactivation of the selected gram-negative (*E. coli* O157:H7) and the gram-positive (*L. innocua*)) bacteria as a function of treatment time in the presence of PG or LFU alone and their combined treatment (PG + LFU). The combined treatment of PG and LFU led to an enhanced bacterial inactivation compared to the individual treatments of PG or LFU ($P < 0.05$). Combined LFU + PG treatment achieved a 6-log reduction in both *E. coli* O157:H7 and *L. innocua* within 30 and 45 min respectively. Meanwhile, the LFU by itself caused no significant reduction in both bacteria. Incubation of *E. coli* O157:H7 cells with PG by itself resulted in about 2-log inactivation of bacteria after 30 min of incubation, while no antimicrobial activity against *L. innocua* was observed after 45 min of incubation. Based on the first-order kinetic model, the kinetic rate constant, k values of 0.51 ± 0.015 and 0.34 ± 0.011 min^{-1} were obtained for the *E. coli* O157:H7 and *L. innocua,* respectively, using the combined treatment. D-values, calculated from these rate constants, were 4.6 ± 0.2 min and 6.88 ± 0.4 min for the *E. coli* O157:H7 and *L. innocua,* respectively ($P < 0.05$). These bacterial inactivation parameters confirmed higher susceptibility of the gram-negative *E. coli* O157:H7 to the combined LFU + PG treatment than the gram-positive *L. innocua*. The difference in susceptibility of *E. coli* O157:H7 and *L. innocua* to the combined treatment could be attributed to differences in the bacterial membrane/cell wall properties and potential differences

Table 1
Size distributions, polydispersity indices (PDI), and ξ potentials of model liposomes in the presence of propyl gallate (PG), after low-frequency ultrasound treatment (LFU), and after the combined treatment of propyl gallate and ultrasound (LFU + PG).

Samples	Avg Size (nm)	PDI	ξ Potential (mV)
Liposome	229.6 ± 57.04	0.152	– 32.7 ± 1.1
Liposome + PG (10 ppm)	225.7 ± 73.6	0.222	– 28.7 ± 0.3
Liposome + LFU (30 min)	178.6 ± 83.6	0.205	– 25.8 ± 1.1
Liposome + PG (10 ppm) + LFU (30 min)	196.9 ± 64.2	0.192	– 27.6 ± 1.2

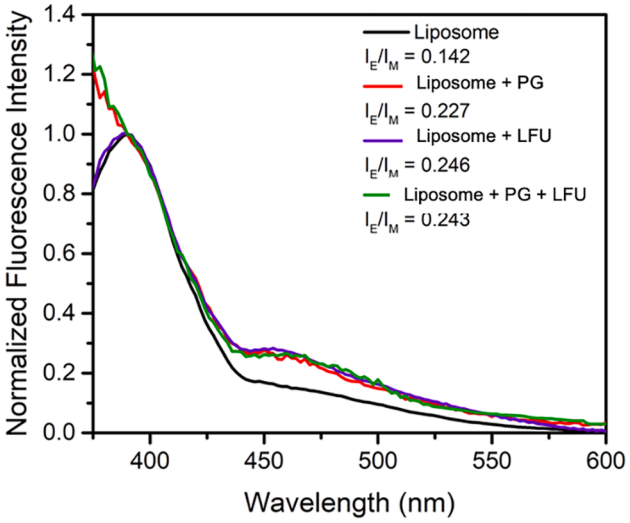

Fig. 3. Normalized fluorescence intensities and the excimer to monomer intensity ratios (I_E/I_M) of β-Py-C10-HPC in liposomes with and without treatments with propyl gallate (PG, 10 mM), low-frequency ultrasound (LFU, 30 min), and combination of LFU + PG.

in interactions between the PG and the bacterial membrane.

The lethal effect caused by conventional LFU treatments in bacterial and mammalian cells has been attributed to a cavitation process [33]. Cavitation can generate mechanical stress on the cell membrane during bubble expansion and contraction and a collapse of bubbles can create a localized shock effect that propels a high-velocity jet of liquid towards the surface. This set of mechanical forces can perforate the bacterial membrane [34] and result in a release of the intracellular components including nucleic acid.

Among possible synergies between PG and LFU, interactions of PG with membranes can further enhance the extent of damage caused by the LFU treatment. PG is known to interact with the bacterial cell membrane [23]. Thus, PG can alter the permeation and fluidity properties of the bacterial membrane.

3.2. Membrane damage

3.2.1. Analysis of membrane damage using model liposomes

To identify the role of membrane damage in the synergistic antimicrobial activity both model liposomes and bacterial cells were evaluated. The use of model liposomes enabled assessment of the influence of PG, LFU, and LFU + PG treatments on the biophysical aspects of the model membrane structure. Previously, we have demonstrated the application of model liposomes to study the synergistic antimicrobial activity of a food-grade peptide with light and mild heat [35]. The structural changes in liposomes cell model membranes induced by PG, LFU, and their combined treatment were evaluated using a combination of particle size and ξ potential measurements, as well as changes in the lateral mobility of model liposomes. The average volume means

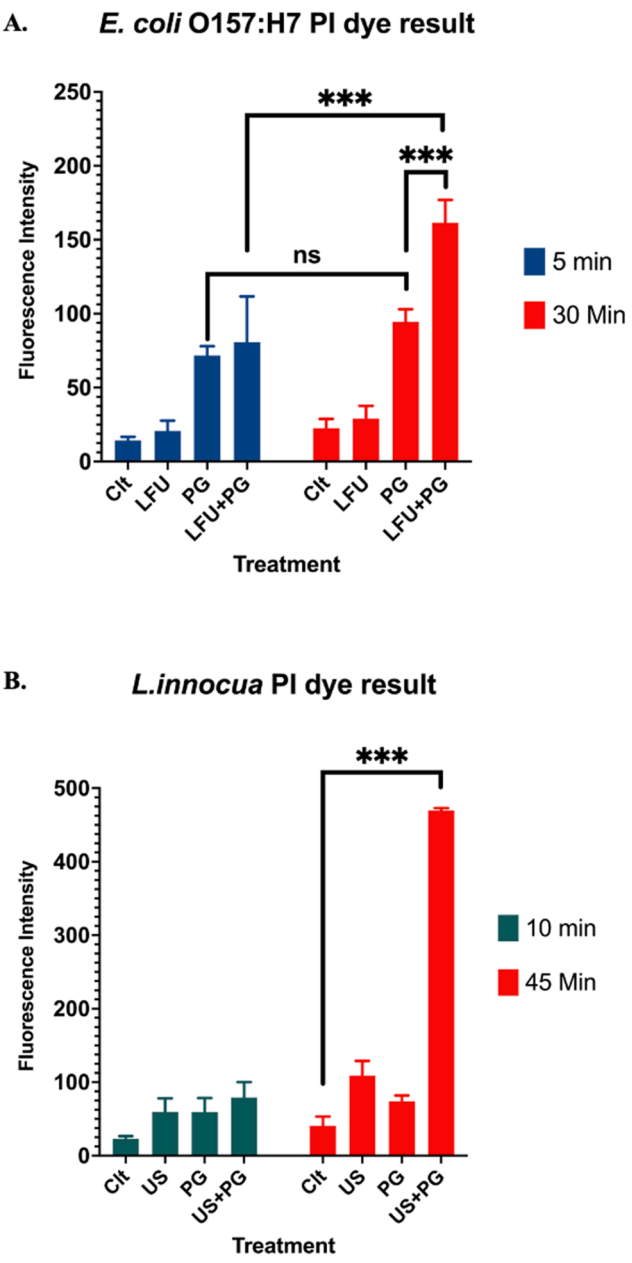

Fig. 4. Relative intracellular PI uptake by bacterial cells as a measure of bacterial membrane integrity after PG, LFU, and LFU + PG treatments of *E. coli* O157:H7 *(A) and L. innocua (B)* for 10 and 45 min.

diameter, polydispersity indices (PDI), and ξ potential of liposomes with and without treatments are shown in Table 1. A low PDI (0.152) and a high zeta potential (– 32.7 mV) demonstrated stable monodisperse unilamellar vesicles with an average particle size of ~230 nm. After treatment with PG, LFU, and LFU + PG, the average diameter of liposomes did not change significantly ($P > 0.05$), and PDI was in the range of 0.15 – 0.2 (Table 1), demonstrating no lysis or flocculation of the liposomes. However, a statistically significant but relatively small reduction in zeta potential was observed ($P < 0.05$) after treatment of liposomes with PG, LFU, and LFU + PG. Statistical analysis also showed no significant change ($P > 0.2$) in ξ potential between liposomes treated with LFU + PG and liposomes with PG or LFU alone.

Emission spectra of β-Py-C10-HPC in liposome displays the pyrene monomer peak at 390 nm and a broad excimer peak at 470 nm [36]. Based on this spectral measurement (supplementary Fig. S1), the excimer to monomer ratio (I_E/I_M) was calculated (Fig. 3). The results show

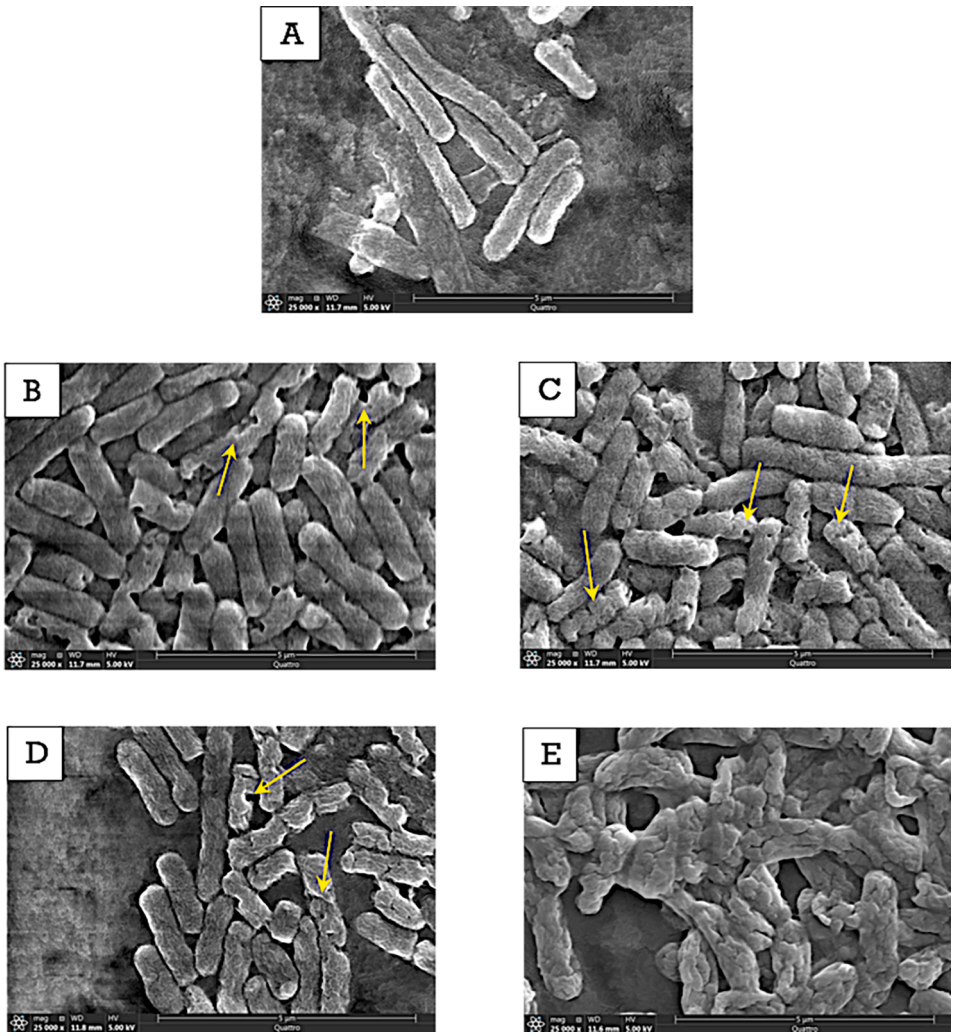

Fig. 5. Scanning electron microscope (SEM) images of ultrasound treated *E. coli* O157:H7 cells: control sample (A), sample which was incubated in PG for 5 min (B), sample which was incubated in PG for 30 min (C), combined LFU + PG treatment for 5 min (D), combined LFU + PG treatment for 30 min (E).

an increase in the lateral mobility of the membrane illustrated by an increase in the excimer to monomer ratio upon treatment with PG, LFU, and a combination of PG + LFU compared to the control liposomes.

Similar to particle size distribution and ξ potential values, combined treatment of PG and LFU did not show significant changes in the β-Py-C10-HPC labeled fluorescence response in comparison to PG or LFU treatment alone. In addition to changes in excimer to monomer ratio, significant fluorescence quenching was also observed in the liposome samples (Supplementary Fig. S1) treated with PG and LFU + PG, illustrating significant interactions of PG with the membrane-associated fluorescence dye and therefore support the plausibility of permeation of PG into the membrane. Overall, these results suggest rapid interactions between PG and model liposomes, however, these interactions did not induce significant lysis of the membrane as observed in our prior study with lauric arginate (LAE) [35].

3.2.2. Analysis of bacterial membrane permeability using PI dye

To complement measurements using liposomes, changes in the bacterial cell membrane upon interactions of LFU and PG were measured using propidium iodide as a membrane permeability indicator. Fig. 3 illustrates changes in the membrane permeability of bacteria upon treatment with PG, LFU, and PG + LFU. For the gram-negative *E. coli* O157:H7, the combined LFU + PG treatments significantly increased the membrane permeability with an increase in treatment time ($P < 0.05$). Meanwhile, treatments with PG alone also generated substantial damage compared to US treatment alone and the control cells. The damage caused by PG was independent of the incubation time. It did not change significantly with an increase in incubation time ($P > 0.05$). In contrast, limited changes in cell permeability were detected for the gram-positive *L. innocua* within the first 10 min of treatment. However, a significant increase in PI permeability was observed after treating for 45 min using a combined LFU + PG treatment ($P < 0.05$).

Using both liposomes and the gram-negative bacterial cells, the results illustrate significant interactions of PG with the membrane. Similar to the results with liposomes, the bacterial cell permeability measurements showed no synergistic increase in membrane permeability with combined treatment of PG and LFU during the first five minutes. The results in Fig. 4-A also show a synergistic increase in the membrane permeability with extended treatment (LFU + PG treatment) for 30 min. Together the results using both liposomal model system and bacterial cells show rapid interactions of PG with lipid membranes based on changes in membrane fluidity and permeability respectively. However, with extended LFU treatment, the PG incubated bacterial cells accumulate a significant increase in the membrane permeability.

A similar trend was also observed in the case of gram-positive *L. innocua* cells. In this case, no synergistic increase in the membrane permeability with PG and LFU was achieved with 10 min of treatment. After a combined treatment of 45 min, an increase in the membrane permeability was observed ($P < 0.001$) as illustrated in Fig. 4-B.

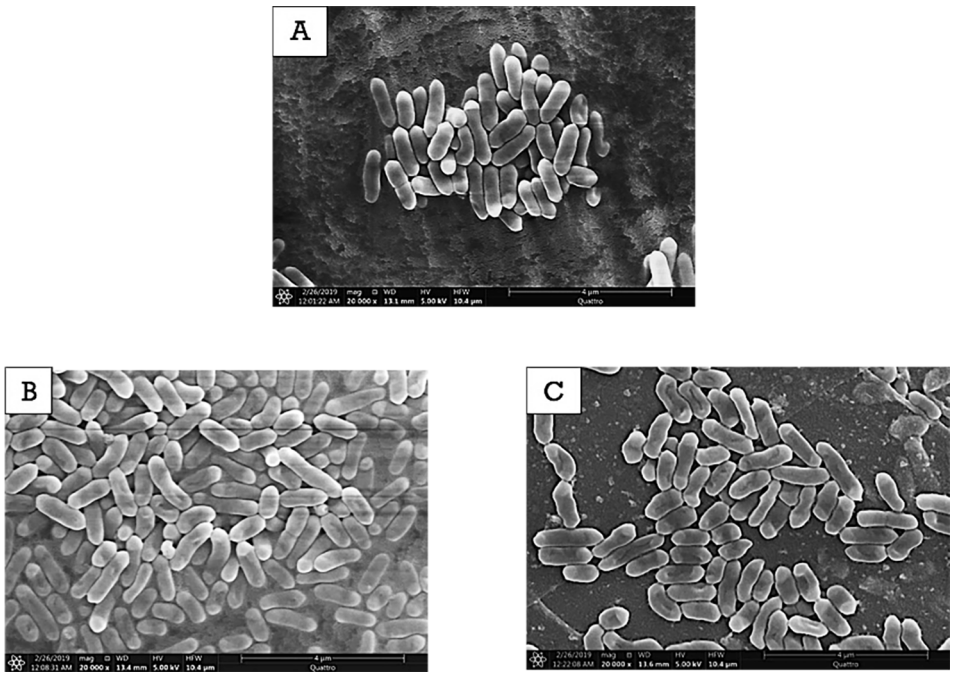

Fig. 6. Scanning electron microscope (SEM) images of ultrasound treated *L.innocua* cells: control sample (A), combined LFU + PG treatment for 10 min (B), combined US + PG treatment for 45 min (C).

Comparison between the gram-negative and the gram-positive results in Fig. 4, also illustrate significant differences in the sensitivity of bacterial cells to the synergistic antimicrobial activity of LFU and the food-grade compound. These differences in susceptibility of bacterial cells can be attributed to the presence of a thicker and a rigid cell wall in the gram-positive bacteria that can reduce susceptibility of the bacteria to PG and its combination with LFU.

3.2.3. SEM figures compare E. coli O157:H7 and L. Innocua cellular morphology change under individual and combined treatment of PG and LFU

Fig. 5 reveals the morphological changes of *E. coli* O157:H7 and *L. innocua* cells after LFU treatment with and without the presence of PG using the SEM technique. In addition, the influence of PG only treatment on cellular morphology was also assessed. After LFU treatment in the presence of PG for 30 min, most *E. coli* O157:H7 cells were severely deformed and notable morphological changes were observed (Fig. 5-E). Ruptured and distorted cell envelopes were also observed. Moreover, it appears that *E. coli* O157:H7 cells were reduced in size probably due to leakage of the intracellular components as a result of the membrane damage. The untreated *E. coli* O157:H7 cells retained the rod-shaped cell morphology with a smooth surface (Fig. 5-A). The images of *E. coli* O157:H7 cells after incubation for 5 and 30 min with PG alone were similar to the images of cells obtained after treatment with the combined LFU + PG treatment for 5 min (Fig. 5-B, C, D). These features include pore formation and localized rupture as highlighted in the Fig. 5-B, C, D. During these treatment conditions, only a fraction of the bacterial cells was influenced, while several cells retained their structure and morphology, similar to the controls. This further highlights the increased membrane damage induced by the combination of LFU + PG is only achieved after extended treatment. These results also support the observations in Figs. 3 and 4 that PG rapidly interacts with lipid membranes. In contrast, cells treated with the combined LFU + PG for an extended period had extensive changes in cellular morphology across the majority of the bacterial cells and these changes were distinct from the results observed in Fig. 5 B-D including fusion of cellular mass.

Fig. 6 describes the morphological changes of *L. innocua* cells after LFU treatment with and without the presence of PG. In contrast to the

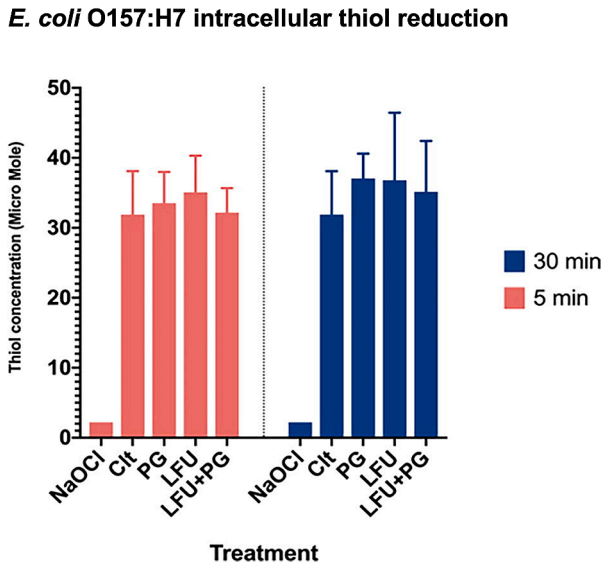

Fig. 7. Intracellular thiol content in *E. coli* O157:H7 cells following treatment with PG, LFU, or LFU + PG for 5 or 30 min. Untreated cells were used as a negative control and sodium hypochlorite (100 ppm) treated cells were used as a positive control.

results with the *E. coli* O157:H7, the combined LFU + PG treatments caused minor changes to the *L. innocua* cell morphology. After LFU + PG treatment for 10 min, most *L. innocua* cells maintained similar cell morphology, but part of the cells showed minor damage (Fig. 6-B). In Fig. 6-C, after 45 min of LFU + PG treatment, concave cell envelopes were observed although the shape of *L.innocua* cells did not change. The pore formation and localized rupture were not observed in *L.innocua* after the treatment. These results in combination with membrane permeability measurements further confirm the higher susceptibility of the gram-negative *E. coli* O157:H7 to the PG and to the combined LFU + PG treatments than the gram-positive *L. innocua*.

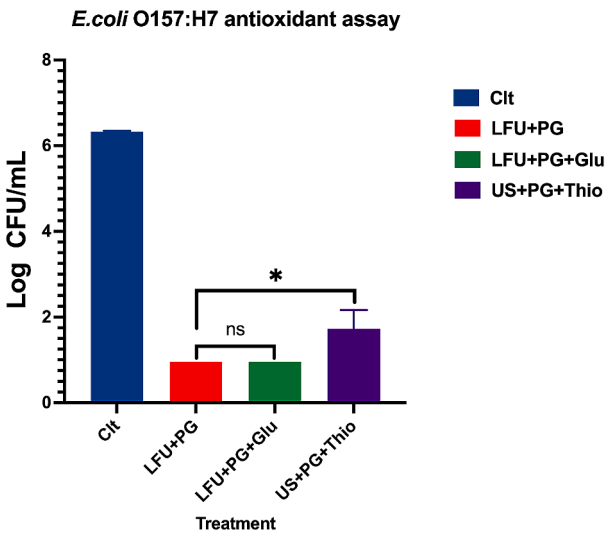

Fig. 8. The effect of antioxidant addition to the combined LFU and PG treatment at 30 min of treatment time where Glu is glutathione and Thio is thiourea.

3.3. Oxidative damage

3.3.1. Total intracellular thiol reduction of E. Coli O157:H7

To evaluate influence of the combined LFU and PG treatment to generate ROS, an endogenous intracellular oxidative stress indicator was utilized. Within the cell cytoplasm, thiol content is a reliable indicator of oxidative stress levels as changes in the thiol content has been correlated with the intracellular ROS formation [23,37–39]. Fig. 7 demonstrates the reduction in the intracellular thiol content of *E. coli* O157:H7 after treatment with LFU in the presence of PG. *E. coli* O157:H7 cells were selected for this assay based on the fact that the intracellular thiol content in *L. innocua* is inherently low [35,40,41], which may limit detection of further reduction in its level after the treatment. There were no significant differences ($P > 0.05$) in the total thiol content among all selected treatments except for the positive controls which were treated with sodium hypochlorite. The results indicate that under the selected conditions, LFU, PG treatment, and the combined LFU + PG treatment did not generate oxidative stress in the cytoplasm, and thus the oxidative damage may not play a significant role in the synergistic bacterial inactivation.

The oxidative stress generation as a result of the sonochemical reactions has been suggested as one of the inactivation mechanisms for the ultrasound treatment [34,42–45]. The ROS can be generated by the transient cavitation processes or it can result from the excitation of exogenous or endogenous cellular components by the ultrasound as well as the localized thermal effects of ultrasound. Cavitation induced ROS generation is one of the most frequently described bactericidal mechanism of ultrasound in the literature [34,46–48]. In this study, the intracellular ROS generation could not be confirmed (Fig. 7). The reason can be attributed to the low energy density of the selected ultrasound treatment. The device used in this study only provides an energy density of 0.092 W/mL, which is low compared to the other high-intensity ultrasound devices that generate more vigorous cavitation.

3.3.2. Evaluation of the role of oxidation in combined LFU + PG synergy by supplementing antioxidants

To further validate the lack of ROS generation by the combined LFU + PG treatment, exogenous antioxidants were added to the solution during treatment as ROS quenchers. It was hypothesized that the addition of ROS quenchers would reduce the bactericidal effect and protect the treated bacteria from the combined treatment. Fig. 8 describes the antimicrobial effect of the combined treatment in the presence of glutathione and thiourea. There was a 5 to 6 log reduction in samples with added exogenous antioxidants. This number of log reduction was equivalent to the LFU + PG treated sample without the presence of ROS quenchers. There was no significant difference ($P > 0.05$) between samples with and without glutathione. There was a small but significant difference between samples with and without thiourea ($P < 0.05$); however, this difference is attributed to the fact that the concentration of thiourea was ten times higher than that of glutathione. In general, the protective effect from the addition of antioxidants was not observed. This observation together with the data from the total intracellular thiol reduction confirms the lack of significant role of ROS in the observed synergistic inactivation of bacteria.

4. Conclusions

Low-frequency ultrasound (LFU) and Propyl Gallate (PG) act synergistically to enhance the inactivation rates of the gram-negative *E. coli* O157:H7 and the gram-positive *L. innocua*. Based on the measurements using both liposomes and bacteria cells, rapid interaction of PG with lipid membranes is one of the key factors for the observed accelerated inactivation of bacteria. This interaction increases lateral mobility in the membrane of liposomes and enhances permeability in the bacterial membrane. In bacterial cells, the combination of LFU with PG increased the membrane permeability with extended treatment time. SEM imaging corroborated with the results obtained from the bacterial membrane damage assay. A lack of significant change in the intracellular thiol content as well as a lack of protective effect from exogenous antioxidants to the antibacterial effect indicate that oxidative stress generation was not a leading mechanism responsible for the enhanced antimicrobial effect. Overall, these results illustrate a novel approach to achieve more than 5 log inactivation of bacteria using a synergistic combination of PG with a low intensity and a low-frequency ultrasound process.

CRediT authorship contribution statement

Cuong Nguyen Huu: Data curation, Writing - original draft. **Rewa Rai:** Data curation, Methodology, Writing - original draft. **Xu Yang:** Methodology, Data curation. **Rohan Tikekar:** Conceptualization, Writing - review & editing, Funding acquisition. **Nitin Nitin:** Conceptualization, Methodology, Writing - review & editing, Funding acquisition.

Declaration of Competing Interest

The authors declare that they have no known competing financial interests or personal relationships that could have appeared to influence the work reported in this paper.

Acknowledgements

This project was supported by the Agriculture and Food Research Initiative by grant no. 2014-67017-21642 from the USDA National Institute of Food and Agriculture (USDA-NIFA) Program in Improving Food Quality (A1361) and by grant no. 2015-68003- 23411 from the USDA-NIFA Program Enhancing Food Safety through Improved Processing Technologies (A4131).

Appendix A. Supplementary data

Supplementary data to this article can be found online at https://doi.org/10.1016/j.ultsonch.2021.105567.

References

[1] M. Ashokkumar, Applications of ultrasound in food and bioprocessing, Ultrason. Sonochem. 25 (2015) 17–23, https://doi.org/10.1016/j.ultsonch.2014.08.012.

[2] F.J. Barba, L. Ahrné, E. Xanthakis, M.G. Landerslev, V. Orlien, Chapter 2. Innovative Technologies for Food Preservation, (2017). doi:10.1016/B978-0-12-811031-7.00002-9.

[3] S. Kentish, H. Feng, Applications of Power Ultrasound in Food Processing, Annu. Rev. Food Sci. Technol. 5 (2014) 263–284, https://doi.org/10.1146/annurev-food-030212-182537.

[4] A. Moody, G. Marx, B.G. Swanson, D. Bermúdez-Aguirre, A comprehensive study on the inactivation of Escherichia coli under nonthermal technologies: High hydrostatic pressure, pulsed electric fields and ultrasound, Food Control. 37 (2014) 305–314, https://doi.org/10.1016/J.FOODCONT.2013.09.052.

[5] A.M. Rediske, B.L. Roeder, M.K. Brown, J.L. Nelson, R.L. Robison, D.O. Draper, G. B. Schaalje, R.A. Robison, W.G. Pitt, Ultrasonic enhancement of antibiotic action on Escherichia coli biofilms: An in vivo model, Antimicrob. Agents Chemother. 43 (1999) 1211–1214, https://doi.org/10.1128/aac.43.5.1211.

[6] A.I.V. Ross, M.W. Griffiths, G.S. Mittal, H.C. Deeth, Combining nonthermal technologies to control foodborne microorganisms, Int. J. Food Microbiol. (2003), https://doi.org/10.1016/S0168-1605(03)00161-2.

[7] H. Hirschberg, S.J. Madsen, Synergistic efficacy of ultrasound, sonosensitizers and chemotherapy: A review, Ther. Deliv. 8 (2017) 331–342, https://doi.org/10.4155/tde-2016-0080.

[8] F. Harris, S.R. Dennison, D.A. Phoenix, Using sound for microbial eradication - light at the end of the tunnel? FEMS Microbiol. Lett. 356 (2014) 20–22, https://doi.org/10.1111/1574-6968.12484.

[9] X. Pang, C. Xu, Y. Jiang, Q. Xiao, A.W. Leung, Natural products in the discovery of novel sonosensitizers, Pharmacol. Ther. 162 (2016) 144–151, https://doi.org/10.1016/J.PHARMTHERA.2015.12.004.

[10] F. Giuntini, F. Foglietta, A.M. Marucco, A. Troia, N.V. Dezhkunov, A. Pozzoli, G. Durando, I. Fenoglio, L. Serpe, R. Canaparo, Insight into ultrasound-mediated reactive oxygen species generation by various metal-porphyrin complexes, Free Radic. Biol. Med. 121 (2018) 190–201, https://doi.org/10.1016/j.freeradbiomed.2018.05.002.

[11] M.M. Rahman, K. Ninomiya, C. Ogino, N. Shimizu, Ultrasound-induced membrane lipid peroxidation and cell damage of Escherichia coli in the presence of non-woven TiO2 fabrics, Ultrason. Sonochem. 17 (2010) 738–743, https://doi.org/10.1016/j.ultsonch.2009.12.001.

[12] X. Wang, A.W. Leung, H. Hua, C. Xu, M. Ip, Sonodynamic action of hypocrellin B on biofilm-producing *Staphylococcus epidermidis* in planktonic condition, J. Acoust. Soc. Am. 138 (2015) 2548–2553, https://doi.org/10.1121/1.4932014.

[13] X. Wang, M. Ip, A.W. Leung, C. Xu, Sonodynamic inactivation of methicillin-resistant Staphylococcus aureus in planktonic condition by curcumin under ultrasound sonication, Ultrasonics. 54 (2014) 2109–2114, https://doi.org/10.1016/j.ultras.2014.06.017.

[14] K. Kajiya, H. Hojo, M. Suzuki, F. Nanjo, S. Kumazawa, T. Nakayama, Relationship between Antibacterial Activity of (+)-Catechin Derivatives and Their Interaction with a Model Membrane, (2004). doi:10.1021/jf0350111.

[15] L.J. Nohynek, H.-L. Alakomi, M.P. Kähkönen, M. Heinonen, I.M. Helander, K.-M. Oksman-Caldentey, R.H. Puupponen-Pimiä, Berry Phenolics: Antimicrobial Properties and Mechanisms of Action Against Severe Human Pathogens, Nutr. Cancer. 54 (2006) 18–32, https://doi.org/10.1207/s15327914nc5401_4.

[16] E.F. De Oliveira, A. Cossu, R. V. Tikekar, N. Nitin, J. Björkroth, E.F. de Oliveira, A. Cossu, R. V. Tikekar, N. Nitin, Enhanced Antimicrobial Activity Based on a Synergistic Combination of Sublethal Levels of Stresses Induced by UV-A Light and Organic Acids, Appl. Environ. Microbiol. 83 (2017) AEM.00383-17. doi:10.1128/AEM.00383-17.

[17] E.F. De Oliveira, A. Cossu, R. V Tikekar, N. Nitin, J. Björkroth, Enhanced Antimicrobial Activity Based on a Synergistic Combination of Sublethal Levels of Stresses Induced by UV-A Light and Organic Acids, (2017). doi:10.1128/AEM.

[18] K. Nakamura, K. Ishiyama, H. Sheng, H. Ikai, T. Kanno, Y. Niwano, Bactericidal Activity and Mechanism of Photoirradiated Polyphenols against Gram-Positive and-Negative Bacteria, (2015). doi:10.1021/jf5058588.

[19] A. Borges, C. Ferreira, M.J. Saavedra, M. Simões, Antibacterial Activity and Mode of Action of Ferulic and Gallic Acids Against Pathogenic Bacteria, Microb. Drug Resist. 19 (2013) 256–265, https://doi.org/10.1089/mdr.2012.0244.

[20] K. Nakamura, Y. Yamada, H. Ikai, T. Kanno, K. Sasaki, Y. Niwano, Bactericidal Action of Photoirradiated Gallic Acid via Reactive Oxygen Species Formation, J. Agric. Food Chem. 60 (2012) 10048–10054, https://doi.org/10.1021/jf303177p.

[21] L. Boyd, E.G. Beveridge, Antimicrobial activity of some alkyl esters of gallic acid (3,4,5,-trihydroxybenzoic acid) against Escherichia coli NCTC 5933 with particular reference to n-propyl gallate, Microbios. 30 (1981) 73–85 (accessed March 7, 2019), http://www.ncbi.nlm.nih.gov/pubmed/6272069.

[22] P. Tammela, L. Laitinen, A. Galkin, T. Wennberg, R. Heczko, H. Vuorela, J.P. Slotte, P. Vuorela, Permeability characteristics and membrane affinity of flavonoids and alkyl gallates in Caco-2 cells and in phospholipid vesicles, Arch. Biochem. Biophys. 425 (2004) 193–199, https://doi.org/10.1016/j.abb.2004.03.023.

[23] Q. Wang, E.F. De Oliveira, S. Alborzi, L.J. Bastarrachea, R.V. Tikekar, On mechanism behind UV-A light enhanced antibacterial activity of gallic acid and propyl gallate against Escherichia coli O157:H7, Sci. Rep. 7 (2017) 1–11, https://doi.org/10.1038/s41598-017-08449-1.

[24] EFSA J. 12 (2014) 3642, https://doi.org/10.2903/j.efsa.2014.3642.

[25] A.H. Geeraerd, V.P. Valdramidis, J.F. Van Impe, GInaFiT, a freeware tool to assess non- log-linear microbial survivor curves, Int. J. Food Microbiol. 102 (2005) 95–105, https://doi.org/10.1016/j.ijfoodmicro.2004.11.038.

[26] T.A. Bigelow, T. Northagen, T.M. Hill, F.C. Sailer, The Destruction of Escherichia Coli Biofilms Using High-Intensity Focused Ultrasound, Ultrasound Med. Biol. 35 (2009) 1026–1031, https://doi.org/10.1016/j.ultrasmedbio.2008.12.001.

[27] H.M. Davey, P. Hexley, Red but not dead? Membranes of stressed Saccharomyces cerevisiae are permeable to propidium iodide, Environ. Microbiol. 13 (2011) 163–171, https://doi.org/10.1111/j.1462-2920.2010.02317.x.

[28] R. Virto, P. Mañas, I. Álvarez, S. Condon, J. Raso, Membrane damage and microbial inactivation by chlorine in the absence and presence of a chlorine-demanding substrate, Appl. Environ. Microbiol. 71 (2005) 5022–5028, https://doi.org/10.1128/AEM.71.9.5022-5028.2005.

[29] M.A. Kohanski, M.A. DePristo, J.J. Collins, Sublethal Antibiotic Treatment Leads to Multidrug Resistance via Radical-Induced Mutagenesis, Mol. Cell. 37 (2010) 311–320, https://doi.org/10.1016/j.molcel.2010.01.003.

[30] D. Farmer, P. Burcham, P. Marin, The ability of thiourea to scavenge hydrogen peroxide and hydroxyl radicals during the intra-coronal bleaching of bloodstained root-filled teeth, Aust. Dent. J. 51 (2006) 146–152, https://doi.org/10.1111/j.1834-7819.2006.tb00418.x.

[31] B.W. Davies, M.A. Kohanski, L.A. Simmons, J.A. Winkler, J.J. Collins, G.C. Walker, Hydroxyurea Induces Hydroxyl Radical-Mediated Cell Death in Escherichia coli, Mol. Cell. 36 (2009) 845–860, https://doi.org/10.1016/j.molcel.2009.11.024.

[32] J.J. Foti, B. Devadoss, J. Winkler, J. Collins, G. Walker, Oxidation of the Guanine Nucleotide Pool Underlies Cell Death by Bactericidal Antibiotics, Science (80-.) 336 (2012) 315–319.

[33] J.E. Repine, R.B. Fox, E.M. Berger, Hydrogen peroxide kills Staphylococcus aureus by reacting with staphylococcal iron to form hydroxyl radical, J. Biol. Chem. 256 (1981) 7094–7096.

[34] P. Piyasena, E. Mohareb, R.C. McKellar, Inactivation of microbes using ultrasound: A review, Int. J. Food Microbiol. 87 (2003) 207–216, https://doi.org/10.1016/S0168-1605(03)00075-8.

[35] M. Erriu, C. Blus, S. Szmukler-Moncler, S. Buogo, R. Levi, G. Barbato, D. Madonnaripa, G. Denotti, V. Piras, G. Orrù, Microbial biofilm modulation by ultrasound: Current concepts and controversies, Ultrason. Sonochem. 21 (2014) 15–22, https://doi.org/10.1016/j.ultsonch.2013.05.011.

[36] X. Yang, R. Rai, C.N. Huu, N. Nitin, Synergistic antimicrobial activity by light or thermal treatment and lauric arginate: Membrane damage and oxidative stress, Appl. Environ. Microbiol. 85 (2019), https://doi.org/10.1128/AEM.01033-19.

[37] Q. Zhang, S.P. Morgan, P. O'Shea, M.L. Mather, Ultrasound induced fluorescence of nanoscale liposome contrast agents, PLoS One. 11 (2016), https://doi.org/10.1371/journal.pone.0159742.

[38] J.R. Terrill, H.G. Radley-Crabb, T. Iwasaki, F.A. Lemckert, P.G. Arthur, M. D. Grounds, Oxidative stress and pathology in muscular dystrophies: Focus on protein thiol oxidation and dysferlinopathies, FEBS J. 280 (2013) 4149–4164, https://doi.org/10.1111/febs.12142.

[39] H. Kundi, I. Ates, E. Kiziltunc, M. Cetin, H. Cicekcioglu, S. Neselioglu, O. Erel, E. Ornek, A novel oxidative stress marker in acute myocardial infarction; Thiol/disulphide homeostasis, Am. J. Emerg. Med. 33 (2015) 1567–1571, https://doi.org/10.1016/j.ajem.2015.06.016.

[40] Z. Lou, P. Li, X. Sun, S. Yang, B. Wang, K. Han, A fluorescent probe for rapid detection of thiols and imaging of thiols reducing repair and H2O2 oxidative stress cycles in living cells, Chem. Commun. 49 (2013) 391–393, https://doi.org/10.1039/c2cc36839k.

[41] J. Sun, Y. Hang, Y. Han, X. Zhang, L. Gan, C. Cai, Z. Chen, Y. Yang, Q. Song, C. Shao, Y. Yang, Y. Zhou, X. Wang, C. Cheng, H. Song, Deletion of glutaredoxin promotes oxidative tolerance and intracellular infection in Listeria monocytogenes, (2019). doi:10.1080/21505594.2019.1685640.

[42] S. Subhra Chatterjee, H. Hossain, S. Otten, C. Kuenne, K. Kuchmina, S. Machata, E. Domann, T. Chakraborty, T. Hain, Intracellular Gene Expression Profile of Listeria monocytogenes †, Infect. Immun. 74 (2006) 1323–1338, https://doi.org/10.1128/IAI.74.2.1323-1338.2006.

[43] A. Demirdöven, T. Baysal, The Use of Ultrasound and Combined Technologies in Food Preservation, Food Rev. Int. 25 (2008) 1–11, https://doi.org/10.1080/87559120802306157.

[44] H. Lee, B. Zhou, W. Liang, H. Feng, S.E. Martin, Inactivation of Escherichia coli cells with sonication, manosonication, thermosonication, and manothermosonication: Microbial responses and kinetics modeling, J. Food Eng. 93 (2009) 354–364 (accessed February 18, 2019), https://www.sciencedirect.com/science/article/pii/S0260877409000636.

[45] S. Gao, G. Lewis, Y. Hemar, Ultrasonic Inactivation of Microorganisms, (n.d.). doi:10.1007/978-981-287-278-4_69.

[46] P. Singh, A. Kumar, N.K. Dubey, R. Gupta, Ultrasound enhanced sanitizer efficacy in reduction of escherichia coli o157:h7 population on spinach leaves, J. Food Sci. 74 (2009) 308–313, https://doi.org/10.1111/j.1750-3841.2009.01223.x.

[47] B. Liu, D.-J. Wang, B.-M. Liu, X. Wang, L.-L. He, J. Wang, S.-K. Xu, The influence of ultrasound on the fluoroquinolones antibacterial activity, (2011). doi:10.1016/j.ultsonch.2011.02.001.

[48] F. Nakonechny, M. Nisnevitch, Y. Nitzan, M. Nisnevitch, Sonodynamic excitation of rose bengal for eradication of gram-positive and gram-negative bacteria, Biomed Res. Int. 2013 (2013), https://doi.org/10.1155/2013/684930.